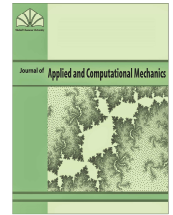




# Journal of Applied and Computational Mechanics



Research Paper

## New Analytical Study for Nanofluid between Two Non-Parallel Plane Walls (Jeffery-Hamel Flow)

Abeer Majeed Jasim

Department of Mathematics, College of Science, University of Basrah, Basrah, Iraq

Received September 08 2020; Revised September 26 2020; Accepted for publication September 28 2020.

Corresponding author: A.M. Jasim (abeer.jassem@yahoo.com)

© 2020 Published by Shahid Chamran University of Ahvaz

**Abstract.** The aim of this paper is to analyze the problem of magneto hydrodynamic Jeffery-Hamel flow (JHF) with nanoparticles. The governing equations for this problem are reduced to an ordinary differential equation and it is solved using new analytical method (NAM) and fourth-order Runge-Kutta Method (RK ~ 4). The NAM is an iterative method that relies mainly on derivatives with Taylor expansion interference. In addition, the velocity profile has been computed and shown for various values of physical parameters. The objective of the present work is to investigate the effect of the angles between the plates, Reynold number, magnetic number and nanoparticles volume fraction on the velocity profile.

**Keywords:** Magneto hydrodynamic flow, Jeffrey-Hamel flow, Nanoparticle, non-linear ordinary differential equation, Analytical solution.

### 1. Introduction

The incompressible viscous fluid flow through convergent-divergent is one of the most applicable cases in fluid mechanics, civil, environmental, mechanical and Bio-mechanical engineering. In fluid dynamics JHF is a flow created by a converging or diverging channel with a source or sink of fluid volume at the point of intersection of the two planes walls. The mathematical investigations of this problem were pioneered by Jeffery [1] and Hamel [2] and so, it is known as Jeffery-Hamel problem. As known, most scientific problems such as Jeffery-Hamel flows and other fluid mechanic problems are inherently nonlinear. In most cases, these problems do not admit analytical solution, so these equations should be solved using special techniques. In recent decades, much attention has been devoted to the newly-developed methods to construct an analytic solution of equation; such as Perturbation techniques which are too strongly dependent upon the so-called small parameters (SP) [3]. Many other different methods have been introduced to solve nonlinear equations [4-22] such as the Adomian decomposition method (ADM), homotopy perturbation method (HPM), variational iteration method (VIM), differential transformation method (DTM), homotopy asymptotic method (HAM) and etc. The main purpose of this study is to apply new analytical method to find approximate analytical solutions (A-AS) of the velocity profile on MHD Jeffery-Hamel flow with nanoparticles. The present article aims at analyzing the problems concerning with the Jeffery-Hamel flow over a convergent-divergent channel in the fluid. The differential equations which represent the Jeffery-Hamel flow between nonparallel walls are nonlinear, therefore, analytical approximations of nonlinear equations are inconceivable. In order to obtain the solutions of the considered problem, we propose a new strategy, Taylor expansion based on a mathematic technique, namely, differential evolution algorithm to analyze show the flow behavior reduces. Furthermore, the competency and reliability of the methods are inspected by employing a fourth -order Runge-Kutta method. The velocity profile is verified graphically through implementation of these two methods. Also, tables are presented for comparing the numerical results at different pertinent parameters. A comparative study has also been done with the previous results and found to be in good compatibility.

**Table 1.** Properties of nanofluid and nanoparticles.

Material	$\rho$ (kg/m <sup>3</sup> )	CP (J/kgK)	k(W/mK)
Al <sub>2</sub> O <sub>3</sub>	3970	765	40
TiO <sub>2</sub>	4250	686.2	8.9538
Cu	8933	385	401
Fluid phase (water)	997.1	4179	0.613



## 2. Mathematical Formulation

We consider the steady two-dimensional flow of an incompressible conducting viscous fluid from a source or sink at the intersection between two nonparallel plane walls. The boundary layer flow of an electrically conducting viscous fluid with nanoparticle is considered. A clear conclusion can be drawn from the numerical method (NUM) results that the NAM provides highly accurate solutions for nonlinear differential equations magnetic field acts transversely to the flow. The problem is described in Figure 1. The velocity is purely radial and depends on  $\tilde{r}$  and  $\tilde{\theta}$  only. The governing equations in polar coordinates follows as [9, 10];

$$\frac{\rho_{nf}}{\tilde{r}} \frac{\partial}{\partial \tilde{r}} (\tilde{r} \hat{u}) = 0, \tag{1a}$$

$$\hat{u} \frac{\partial \hat{u}}{\partial \tilde{r}} + \frac{1}{\rho_{nf}} \frac{\partial p}{\partial \tilde{r}} - \nu_{nf} \left[ \frac{\partial^2 \hat{u}}{\partial \tilde{r}^2} - \frac{1}{\tilde{r}} \frac{\partial \hat{u}}{\partial \tilde{r}} - \frac{1}{\tilde{r}} \frac{\partial^2 \hat{u}}{\partial \tilde{r}^2} + \frac{\hat{u}}{\tilde{r}} \right] + \frac{\sigma M_0^2}{\rho_{nf} \tilde{r}} \hat{u} = 0, \tag{1b}$$

$$\frac{1}{\rho_{nf} \tilde{r}} \frac{\partial p}{\partial \tilde{\theta}} - \frac{2\nu_{nf}}{\tilde{r}^2} \frac{\partial \hat{u}}{\partial \tilde{\theta}} = 0, \tag{1c}$$

where  $M_0$  is the electromagnetic induction,  $\hat{u}$  is the velocity along radial direction,  $p$  is fluid pressure,  $\sigma$  is the conductivity of the fluid,  $\rho_{nf}$  is the density of fluid and  $\nu_{nf}$  is the coefficient of kinematic viscosity. By presenting  $\phi$  as a solid volume fraction, fluid density, dynamic viscosity and the kinematic viscosity of nanofluid can be written as follows:

$$\rho_{nf} = \rho_f(1 - \phi) + \rho_s\phi, \tag{2a}$$

$$\mu_{nf} = \frac{\mu_f}{(1 - \phi)^{2.5}}, \tag{2b}$$

$$\nu_{nf} = \frac{\mu_f}{\rho_{nf}}, \tag{2c}$$

By using dimensionless parameters and from Equation (1a)

$$\hat{f}(\theta) = \hat{u}(\tilde{r}, \tilde{\theta}), \tag{3a}$$

$$\tilde{f}(\eta) = \frac{\hat{f}(\theta)}{\hat{f}_{max}}, \eta = \frac{\theta}{\alpha}, \tag{3b}$$

Substituting Equation (2b) into Equations (1b) and (1c), we obtain an ordinary differential equation for the velocity profile  $f(\eta)$ :

$$\frac{d^3 \tilde{f}}{d\eta^3} + 2\alpha Re \left( (1 - \phi) + \frac{\rho_s}{\rho_f} \phi \right) (1 - \phi)^{2.5} \tilde{f} \frac{d\tilde{f}}{d\eta} + (4 - (1 - \phi)^{1.25} Ha) \alpha^2 \frac{d\tilde{f}}{d\eta} = 0, \tag{4}$$

the subject boundary conditions as follows;

$$\tilde{f}(0) = 0, \frac{d\tilde{f}(0)}{d\eta} = 0, \tilde{f}(1) = 0, \tag{5}$$

the Hartmann and Reynold numbers respectively are

$$Ha = \sqrt{\frac{\sigma M_0^2}{\rho \nu}}, Re = \frac{\hat{f}_{max} \alpha}{\nu} \left( \begin{array}{l} \text{divergentschanel (DC): } \alpha > 0, \hat{f}_{max} > 0 \\ \text{convergschanal (CC): } \alpha < 0, \hat{f}_{max} < 0 \end{array} \right) \tag{6}$$

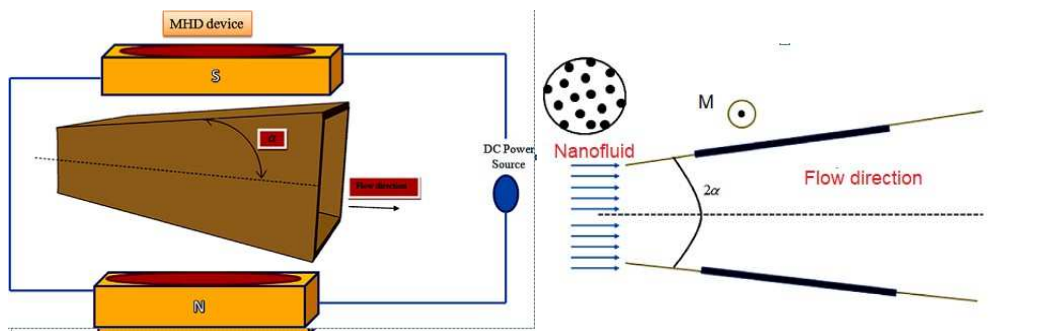


Fig. 1. The nanofluid JHF (a) 2D view and (b) schematic setup of problem.



### 3. The Basic Steps of the New Analytical Method

In this section, review of the basic steps of the NAM is presented. We start by considering the following differential equation:

$$B\left(\eta, \frac{d\tilde{f}(\eta)}{d\eta}, \frac{d^2\tilde{f}(\eta)}{d\eta^2}, \frac{d^3\tilde{f}(\eta)}{d\eta^3}, \dots, \frac{d^{n-1}\tilde{f}(\eta)}{d\eta^{n-1}}, \frac{d^n\tilde{f}(\eta)}{d\eta^n}\right) = 0, \tag{7}$$

where  $B$  is a differential operator,  $\tilde{f}$  is an unknown function,  $\eta$  is an independent variable. Rewriting Equation (3.1) as follows

$$L(\tilde{f}(\eta)) + J(\tilde{f}(\eta)) + N(\tilde{f}(\eta)) + g(\eta) = 0, \tag{8}$$

where  $L$  is the highest-order derivative which is assumed to be invertible,  $J$  is a linear differential operator of less order than  $L$ ,  $N$  represents the nonlinear terms and  $g(\eta)$  is a known analytical function. The series approximate-analytical solution is

$$\tilde{f}(\eta) = \sum_{m=0}^{\infty} \tilde{f}_m(\eta), \tag{9}$$

Integrating Equation (8) with respect to  $\eta$  on  $[0, \eta]$  yields

$$\tilde{f}(\eta) = \sum_{i=0}^{n-1} \tilde{f}^{(i)}(0) \frac{\eta^i}{i!} + L^{-1}g(\eta) + L^{-1}J[\tilde{f}(\eta)] + L^{-1}G[\tilde{f}(\eta)], \tag{10}$$

where,

$$G[\tilde{f}(\eta)] = N(\tilde{f}(\eta)), L^{-1} = \int_0^\eta \int_0^\eta \dots \int_0^\eta (d\eta)^n, \tag{11}$$

where  $n-1$  for the series solution, can be easily be found by the following recursive process:

$$\tilde{f}_0(\eta) = \sum_{i=0}^{n-1} \tilde{f}^{(i)}(0) \frac{\eta^i}{i!} + L^{-1}g(\eta), \tag{12}$$

$$G_0[\tilde{f}(\eta)] = N[\tilde{f}(\eta)] \tag{13}$$

$$\tilde{f}_1(\eta) = L^{-1}J[\tilde{f}_0(\eta)] + G_{0s}L^{-1}[\tilde{f}(\eta)], \tag{14}$$

$$\tilde{f}_{m+1}(\eta) = L^{-1}J[\tilde{f}_m(\eta)] + G_mL^{-1}[\tilde{f}(\eta)], \quad m = 1, 2, \dots,$$

Assume that

$$G_m[\tilde{f}(\eta)] = \sum_{n=0}^m \frac{(\Delta\eta)^n d^n N(\tilde{f}_0(\eta))}{n!} - \sum_{n=0}^{m-1} \frac{(\Delta\eta)^n d^n N(\tilde{f}_0(\eta))}{n!}, \quad m = 1, 2, \dots, \tag{15}$$

Substituting equation (15) in equation (14), we obtain

$$\begin{aligned} \tilde{f}_{m+1}(\eta) &= L^{-1}J[\tilde{f}_m(\eta)] + L^{-1}\left(\sum_{n=0}^m \frac{(\Delta\eta)^n d^n N(\tilde{f}_0(\eta))}{n!} - \sum_{n=0}^{m-1} \frac{(\Delta\eta)^n d^n N(\tilde{f}_0(\eta))}{n!}\right), \\ \tilde{f}_2(\eta) &= L^{-1}J[\tilde{f}_1(\eta)] + L^{-1}\frac{(\Delta\eta)^1 dN(\tilde{f}_0(\eta))}{1!}, \tilde{f}_3(\eta) = L^{-1}J[\tilde{f}_2(\eta)] + L^{-1}\frac{(\Delta\eta)^2 d^2N(\tilde{f}_0(\eta))}{2!}, \end{aligned} \tag{16}$$

$$\tilde{f}_4(\eta) = L^{-1}J[\tilde{f}_3(\eta)] + L^{-1}\frac{(\Delta\eta)^3 d^3N(\tilde{f}_0(\eta))}{3!}, \dots, \tilde{f}_m(\eta) = L^{-1}J[\tilde{f}_{m-1}(\eta)] + L^{-1}\frac{(\Delta\eta)^{m-1} d^{m-1}N(\tilde{f}_0(\eta))}{(m-1)!}$$

We focus on computing the derivatives of  $N$  with respect to  $\eta$  which is the crucial part of the proposed method. Let's start calculating  $N[\tilde{f}(\eta)], N'[\tilde{f}(\eta)], N''[\tilde{f}(\eta)], \dots,$

$$N[\tilde{f}(\eta)] = \left(\tilde{f}(\eta), \frac{d\tilde{f}(\eta)}{d\eta}, \frac{d^2\tilde{f}(\eta)}{d\eta^2}, \frac{d^3\tilde{f}(\eta)}{d\eta^3}, \dots, \frac{d^{n-1}\tilde{f}(\eta)}{d\eta^{n-1}}, \frac{d^n\tilde{f}(\eta)}{d\eta^n}\right), \tag{17}$$

$$N'[\tilde{f}(\eta)] = \sum_{i=1}^n N_{\tilde{f}^{(i-1)}}(\tilde{f}_\eta)^{(i-1)}, \tag{18}$$



$$N''[\tilde{f}(\eta)] = \sum_{j=1}^n \sum_{i=1}^n N_{\tilde{f}^{(j-1)}\tilde{f}^{(i-1)}}(\tilde{f}_\eta)^{(j-1)}(\tilde{f}_\eta)^{(i-1)} + \sum_{i=1}^n N_{\tilde{f}^{(i-1)}}(\tilde{f}_{\eta\eta})^{(i-1)}, \tag{19}$$

$$N'''[\tilde{f}(\eta)] = \sum_{k=1}^n \sum_{j=1}^n \sum_{i=1}^n N_{\tilde{f}^{(k-1)}\tilde{f}^{(j-1)}\tilde{f}^{(i-1)}}(\tilde{f}_\eta)^{(k-1)}(\tilde{f}_\eta)^{(j-1)}(\tilde{f}_\eta)^{(i-1)} + \sum_{j=1}^n \sum_{i=1}^n N_{\tilde{f}^{(j-1)}\tilde{f}^{(i-1)}}(\tilde{f}_{\eta\eta})^{(j-1)}(\tilde{f}_{\eta\eta})^{(i-1)} + \sum_{i=1}^n N_{\tilde{f}^{(i-1)}}(\tilde{f}_{\eta\eta\eta})^{(i-1)}, \tag{20}$$

We see that the calculations become more complicated in the second and third derivatives because of the numerous calculations. Consequently, the systematic structure on calculation is extremely important. Fortunately, due to the assumption that the operator  $N$  and the solution  $\tilde{f}$  are analytic functions then the mixed derivatives are equivalent. We note that the derivative function to  $f$  is unknown, so we suggest the following hypothesis:

$$\begin{aligned} \tilde{f}_\eta &= \tilde{f}_1(\eta) = L^{-1}J[\tilde{f}_0(\eta)] + L^{-1}N[\tilde{f}_0(\eta)], \\ \tilde{f}_{\eta\eta} &= \tilde{f}_2(\eta) = L^{-1}J[\tilde{f}_1(\eta)] + L^{-1}\frac{(\Delta\eta)^1}{1!}N'[\tilde{f}_0(\eta)], \\ \tilde{f}_{\eta\eta\eta} &= \tilde{f}_3(\eta) = L^{-1}J[\tilde{f}_2(\eta)] + L^{-1}\frac{(\Delta\eta)^2}{2!}N''[\tilde{f}_0(\eta)], \\ \tilde{f}_{\eta\eta\eta\eta} &= \tilde{f}_4(\eta) = L^{-1}J[\tilde{f}_3(\eta)] + L^{-1}\frac{(\Delta\eta)^3}{3!}N'''[\tilde{f}_0(\eta)], \\ &\vdots \end{aligned} \tag{21}$$

Therefore equations (12) to (15) are evaluated

$$N[\tilde{f}_0(\eta)] = \left( \tilde{f}(\eta), \frac{d\tilde{f}_0(\eta)}{d\eta}, \frac{d^2\tilde{f}_0(\eta)}{d\eta^2}, \frac{d^3\tilde{f}_0(\eta)}{d\eta^3}, \dots, \frac{d^{n-1}\tilde{f}_0(\eta)}{d\eta^{n-1}}, \frac{d^n\tilde{f}_0(\eta)}{d\eta^n} \right), \tag{22}$$

$$N'[\tilde{f}_0(\eta)] = \sum_{i=1}^n N_{\tilde{f}_0^{(i-1)}}(\tilde{f}_1)^{(i-1)}, \tag{23}$$

$$N''[\tilde{f}_0(\eta)] = \sum_{j=1}^n \sum_{i=1}^n N_{\tilde{f}_0^{(j-1)}\tilde{f}_0^{(i-1)}}(\tilde{f}_1)^{(j-1)}(\tilde{f}_1)^{(i-1)} + \sum_{i=1}^n N_{\tilde{f}_0^{(i-1)}}(\tilde{f}_2)^{(i-1)}, \tag{24}$$

$$N'''[\tilde{f}_0(\eta)] = \sum_{k=1}^n \sum_{j=1}^n \sum_{i=1}^n N_{\tilde{f}_0^{(k-1)}\tilde{f}_0^{(j-1)}\tilde{f}_0^{(i-1)}}(\tilde{f}_1)^{(k-1)}(\tilde{f}_1)^{(j-1)}(\tilde{f}_1)^{(i-1)} + \sum_{j=1}^n \sum_{i=1}^n N_{\tilde{f}_0^{(j-1)}\tilde{f}_0^{(i-1)}}(\tilde{f}_2)^{(j-1)}(\tilde{f}_2)^{(i-1)} + \sum_{i=1}^n N_{\tilde{f}_0^{(i-1)}}(\tilde{f}_3)^{(i-1)}, \tag{25}$$

Substitution Equations (22)-(25) in Equation (9), the required analytical approximate solution for the Equation (7) can be achieved.

### 4. The Application of NAM for JHF with Nanoparticles

The NIM described in the previous section is implemented for solving third or- der nonlinear differential Equations (4) can be consider from the required information as follows

$$J[\tilde{f}(\eta)] = (4 - (1 - \phi)^{1.25}Ha)\alpha^2 \frac{d\tilde{f}(\eta)}{d\eta}, G[\tilde{f}(\eta)] = 2\alpha Re \left( (1 - \phi) + \frac{\rho_s}{\rho_f}\phi \right) (1 - \phi)^{2.5} \tilde{f}(\eta) \frac{d\tilde{f}(\eta)}{d\eta}, \tag{26}$$

$$g(\eta) = 0, L^{-1} = \int_0^\eta \int_0^\eta \int_0^\eta (d\eta)^3,$$

The solution of the given equation involves the extraction of the components of  $\tilde{f}(\eta)$  and the study of the effect of the parameters on them. So solving the approximate analytical series be as listed

$$\tilde{f}(\eta) = \tilde{f}_0(\eta) + \tilde{f}_1(\eta) + \tilde{f}_2(\eta) + \dots, \tag{27}$$

initial conditions are used when the inverse operator  $L^{-1}$  is applied on Equation (27) to obtain

$$\tilde{f}_0(\eta) = \zeta_0 + \zeta_1\eta + \zeta_2 \frac{\eta^2}{2!}, \tag{28}$$

whereas

$$\tilde{f}(0) = \zeta_0, \tilde{f}'(0) = \zeta_1, \tilde{f}''(0) = \zeta_2, \tag{29}$$

for the components of  $f(\eta)$ , can be easily be found by the following iterative



$$\tilde{f}_0(\eta) = 1 + \zeta_2 \frac{\eta^2}{2!}, \tag{30}$$

$$\tilde{f}_1(\eta) = (4 - (1 - \phi)^{1.25} Ha) \alpha^2 \frac{d\tilde{f}_0}{d\eta} + 2\alpha Re \left( (1 - \phi) + \frac{\rho_s}{\rho_f} \phi \right) (1 - \phi)^{2.5} \tilde{f}_0(\eta) \frac{d\tilde{f}_0}{d\eta}, \tag{31}$$

$$\tilde{f}_2(\eta) = (4 - (1 - \phi)^{1.25} Ha) \alpha^2 \frac{d\tilde{f}_1}{d\eta} + L^{-1} \frac{(\Delta\eta)^1}{1!} \frac{dN[\tilde{f}_0]}{d\eta}, \tag{32}$$

$$\tilde{f}_3(\eta) = (4 - (1 - \phi)^{1.25} Ha) \alpha^2 \frac{d\tilde{f}_2}{d\eta} + L^{-1} \frac{(\Delta\eta)^2}{2!} \frac{d^2 N[\tilde{f}_0]}{d\eta^2}, \tag{33}$$

$$\tilde{f}_4(\eta) = (4 - (1 - \phi)^{1.25} Ha) \alpha^2 \frac{d\tilde{f}_3}{d\eta} + L^{-1} \frac{(\Delta\eta)^3}{3!} \frac{d^3 N[\tilde{f}_0]}{d\eta^3}, \tag{34}$$

$$\tilde{f}_5(\eta) = (4 - (1 - \phi)^{1.25} Ha) \alpha^2 \frac{d\tilde{f}_4}{d\eta} + L^{-1} \frac{(\Delta\eta)^4}{4!} \frac{d^4 N[\tilde{f}_0]}{d\eta^4}, \tag{35}$$

Now, we start the calculation of the derivatives of N with respect to  $\eta$  which considers on the basis of

$$N[\tilde{f}(\eta)] = \left( \tilde{f}(\eta), \frac{d\tilde{f}(\eta)}{d\eta}, \frac{d^2\tilde{f}(\eta)}{d\eta^2}, \frac{d^3\tilde{f}(\eta)}{d\eta^3}, \dots, \frac{d^{n-1}\tilde{f}(\eta)}{d\eta^{n-1}}, \frac{d^n\tilde{f}(\eta)}{d\eta^n} \right), \tag{36}$$

$$N'[\tilde{f}(\eta)] = \sum_{i=1}^n N_{\tilde{f}^{(i-1)}}(\tilde{f}_\eta)^{(i-1)}, \tag{37}$$

$$N''[\tilde{f}(\eta)] = \sum_{j=1}^n \sum_{i=1}^n N_{\tilde{f}^{(j-1)}\tilde{f}^{(i-1)}}(\tilde{f}_\eta)^{(j-1)}(\tilde{f}_\eta)^{(i-1)} + \sum_{i=1}^n N_{\tilde{f}^{(i-1)}}(\tilde{f}_{\eta\eta})^{(i-1)}, \tag{38}$$

$$N'''[\tilde{f}(\eta)] = \sum_{k=1}^n \sum_{j=1}^n \sum_{i=1}^n \sum_{l=1}^n N_{\tilde{f}^{(k-1)}\tilde{f}^{(j-1)}\tilde{f}^{(i-1)}}(\tilde{f}_\eta)^{(k-1)}(\tilde{f}_\eta)^{(j-1)}(\tilde{f}_\eta)^{(i-1)} + \sum_{j=1}^n \sum_{i=1}^n N_{\tilde{f}^{(j-1)}\tilde{f}^{(i-1)}}(\tilde{f}_{\eta\eta})^{(j-1)}(\tilde{f}_{\eta\eta})^{(i-1)} + \sum_{i=1}^n N_{\tilde{f}^{(i-1)}}(\tilde{f}_{\eta\eta\eta})^{(i-1)}, \tag{39}$$

We note that the derivatives of  $\tilde{f}$  with respect  $\eta$  that are given in (21), can be computed by Equations (36)-(39) as

$$N[\tilde{f}_0(\eta)] = \left( \tilde{f}_0(\eta), \frac{d\tilde{f}_0(\eta)}{d\eta}, \frac{d^2\tilde{f}_0(\eta)}{d\eta^2}, \frac{d^3\tilde{f}_0(\eta)}{d\eta^3}, \dots, \frac{d^{n-1}\tilde{f}_0(\eta)}{d\eta^{n-1}}, \frac{d^n\tilde{f}_0(\eta)}{d\eta^n} \right), \tag{40}$$

$$N'[\tilde{f}_0(\eta)] = \sum_{i=1}^n N_{\tilde{f}_0^{(i-1)}}(\tilde{f}_1)^{(i-1)}, \tag{41}$$

$$N''[\tilde{f}_0(\eta)] = \sum_{j=1}^n \sum_{i=1}^n N_{\tilde{f}_0^{(j-1)}\tilde{f}_0^{(i-1)}}(\tilde{f}_1)^{(j-1)}(\tilde{f}_1)^{(i-1)} + \sum_{i=1}^n N_{\tilde{f}_0^{(i-1)}}(\tilde{f}_2)^{(i-1)}, \tag{42}$$

$$N'''[\tilde{f}_0(\eta)] = \sum_{k=1}^n \sum_{j=1}^n \sum_{i=1}^n \sum_{l=1}^n N_{\tilde{f}_0^{(k-1)}\tilde{f}_0^{(j-1)}\tilde{f}_0^{(i-1)}}(\tilde{f}_1)^{(k-1)}(\tilde{f}_1)^{(j-1)}(\tilde{f}_1)^{(i-1)} + \sum_{j=1}^n \sum_{i=1}^n N_{\tilde{f}_0^{(j-1)}\tilde{f}_0^{(i-1)}}(\tilde{f}_2)^{(j-1)}(\tilde{f}_2)^{(i-1)} + \sum_{i=1}^n N_{\tilde{f}_0^{(i-1)}}(\tilde{f}_3)^{(i-1)}, \tag{43}$$

After performing NAM, we will obtain the required approximate analytical solution for Equation (4).

### 5. Analysis of the Convergence

We study the analysis of convergence (AC) for the analytical approximate solution (AAS) that are resulted from the application of new power series approach for solving the problem of MHD squeezing fluid flow between two parallel plates in porous medium with slip boundary.



**Definition 5.1.** Suppose that  $H$  is Banach space,  $\mathcal{R}$  is the real numbers and  $G[\tilde{f}]$  is a nonlinear operator defined by  $G[\tilde{f}]:H \rightarrow \mathcal{R}$ , then the sequence of the solutions generated by a NAM can be written as

$$\tilde{f}_{n+1} = K[\tilde{f}_n], K[\tilde{f}_n] = J[\tilde{f}_n] + G[\tilde{f}_n], \tilde{f}_n = \sum_{k=0}^n \tilde{f}_k, n = 0,1,2, \dots, \tag{44}$$

where  $k[\tilde{f}]$  satisfies Lipschitz condition (LC) such that for  $\varphi > 0, \varphi$  in  $\mathcal{R}$ , we have

$$\|K[\tilde{f}_n] - K[\tilde{f}_{n-1}]\| \leq \varphi \|\tilde{f}_n - \tilde{f}_{n-1}\|, \tag{45}$$

**Theorem 5.1.** Let series  $\tilde{f}(\eta) = \sum_{k=0}^{\infty} \tilde{f}_k(\eta)$  is AAS generated by NAM converge if the following condition is satisfied:

$$\|\tilde{f}_n - \tilde{f}_m\| \rightarrow 0, \text{ as } m \rightarrow \infty \text{ for } 0 \leq \varphi < 1$$

**Proof.** From the above definition, we have

$$\begin{aligned} \|\tilde{f}_n - \tilde{f}_m\| &= \left\| \sum_{k=0}^n \tilde{f}_k - \sum_{k=0}^m \tilde{f}_k \right\| \\ &= \left\| \tilde{f}_0 + \sum_{k=0}^{n-1} (L^{-1}J[\tilde{f}_k(\eta)] + L^{-1}G_k[\tilde{f}_k(\eta)]) - \tilde{f}_0 + \sum_{k=0}^{m-1} (L^{-1}J[\tilde{f}_k(\eta)] + L^{-1}G_k[\tilde{f}_k(\eta)]) \right\| \\ &= \left\| \sum_{k=0}^{n-1} L^{-1}J[\tilde{f}_k(\eta)] + L^{-1}(L^{-1}(\sum_{k=0}^{n-1} \frac{(\Delta\eta)^k d^k N(\tilde{f}_0(\eta))}{k!} - \sum_{n=0}^{n-2} \frac{(\Delta\eta)^k d^k N(\tilde{f}_0(\eta))}{k!})) \right. \\ &\quad \left. - \sum_{k=0}^{m-1} L^{-1}J[\tilde{f}_k(\eta)] + L^{-1}(L^{-1}(\sum_{k=0}^{m-1} \frac{(\Delta\eta)^k d^k N(\tilde{f}_0(\eta))}{k!} - \sum_{n=0}^{m-2} \frac{(\Delta\eta)^k d^k N(\tilde{f}_0(\eta))}{k!})) \right\| \\ &= \left\| [L^{-1}k[\sum_{k=0}^{n-1} \tilde{f}_k]] - [L^{-1}k[\sum_{k=0}^{m-1} \tilde{f}_k]] \right\| \\ &\leq |L^{-1}| \|k[\sum_{k=0}^{n-1} \tilde{f}_k] - k[\sum_{k=0}^{m-1} \tilde{f}_k]\| \\ &\leq |L^{-1}| \|k[\tilde{f}_{n-1}] - k[\tilde{f}_{m-1}]\| \\ &\leq \varphi \|\tilde{f}_{n-1} - \tilde{f}_{m-1}\| \end{aligned}$$

since  $K[\tilde{f}]$  satisfies LC. Let  $n = m + 1$ , then

$$\|\tilde{f}_n - \tilde{f}_m\| \leq \varphi \|\tilde{f}_{n-1} - \tilde{f}_{m-1}\|, \tag{46}$$

Hence

$$\|\tilde{f}_m - \tilde{f}_{m-1}\| \leq \varphi \|\tilde{f}_{m-1} - \tilde{f}_{m-2}\| \leq \dots \leq \varphi^{m-1} \|\tilde{f}_1 - \tilde{f}_0\|, \tag{47}$$

from Equation (47), we get

$$\begin{aligned} \|\tilde{f}_2 - \tilde{f}_1\| &\leq \varphi \|\tilde{f}_1 - \tilde{f}_0\|, \\ \|\tilde{f}_3 - \tilde{f}_2\| &\leq \varphi^2 \|\tilde{f}_1 - \tilde{f}_0\|, \\ \|\tilde{f}_4 - \tilde{f}_3\| &\leq \varphi^3 \|\tilde{f}_1 - \tilde{f}_0\|, \\ &\vdots \\ \|\tilde{f}_m - \tilde{f}_{m-1}\| &\leq \varphi^m \|\tilde{f}_1 - \tilde{f}_0\|, \end{aligned}$$

Using triangle equality

$$\begin{aligned} \|\tilde{f}_n - \tilde{f}_m\| &= \|\tilde{f}_n - \tilde{f}_{n-1} - \tilde{f}_{n-2} - \dots - \tilde{f}_{m+1} - \tilde{f}_m\| \\ &\leq \|\tilde{f}_n - \tilde{f}_{n-1}\| + \|\tilde{f}_{n-1} - \tilde{f}_{n-2}\| + \dots + \|\tilde{f}_{m+1} - \tilde{f}_m\| \\ &\leq [\varphi^{n-1} + \varphi^{n-2} + \dots + \varphi^m] \|\tilde{f}_1 - \tilde{f}_0\|, \\ &= \varphi^m [\varphi^{n-m-1} + \varphi^{n-m-2} + \dots + 1] \|\tilde{f}_1 - \tilde{f}_0\|, \\ &\leq \frac{\varphi^m}{1 - \varphi} \|\tilde{f}_1 - \tilde{f}_0\|, \end{aligned}$$



**Table 2.** The values of  $\phi$  by using condition convergence.

	$\rho_s = 3970, Ha = 0, Re = 10, \alpha = 3, \phi = 0.01$	$\rho_s = 8933, Ha = 600, Re = 30, \alpha = 5, \phi = 0.02$		
	$\  \cdot \ _2$	$\  \cdot \ _\infty$	$\  \cdot \ _2$	$\  \cdot \ _\infty$
$\phi$	0.04368886675	0.036811329680	0.03486541970	0.03750562458
$\phi^2$	0.00103423553	0.000955994608	0.00200575022	0.00205646732
$\phi^3$	0.00001848515	0.000015704533	0.00018352086	0.00018579125
$\vdots$	$\vdots$	$\vdots$	$\vdots$	$\vdots$

**Table 3.** The convergence of B3 when  $Ha = 0, Re = 10, \alpha = 3, \phi = 0.01$ .

Approximation	$Al_2O_3$	$TiO_2$	$Cu$
	B3	B3	B3
1 order	-2.1497888	-2.1502136	-2.15733520
2 order	-2.1470085	-2.1474182	-2.15428091
3 order	-2.1469425	-2.1473516	-2.15420414
4 order	-2.1469438	-2.1473528	-2.15420567
5 order	-2.1469438	-2.1473528	-2.15420567
6 order	-2.1469438	-2.1473528	-2.15420567

**Table 4.** The convergence of B3 when  $Ha = 600, Re = 30, \alpha = 5, \phi = 0.02$ .

Approximation	$Al_2O_3$	$TiO_2$	$Cu$
	B3	B3	B3
1 order	-1.96940561	-1.97275131	-2.029852
2 order	-1.97099525	-1.97454545	-2.034925
3 order	-1.97101228	-1.97456162	-2.034842
4 order	-1.97101201	-1.97456126	-2.034738
5 order	-1.97101201	-1.97456126	-2.034738
6 order	-1.97101201	-1.97456126	-2.034738

**5.1. Convergence of the Solution for JHF with Nanoparticles**

In practice, the theorem (5.1) suggests to compute the value of  $\phi$  as described in the following definition

**Definition 5.2.** For  $j= 1, 2, 3, \dots$

$$\phi^j = \begin{cases} \frac{\|\tilde{f}_{j+1} - \tilde{f}_j\|}{\|\tilde{f}_1 - \tilde{f}_0\|}, & \|\tilde{f}_1 - \tilde{f}_0\| \neq 0 \\ 0, & \|\tilde{f}_1 - \tilde{f}_0\| = 0 \end{cases}$$

Note that the Definition (5.2) of convergence condition is achieved through applying it on MHD squeezing fluid flow between two parallel plates in porous medium with slip boundary to find convergence, the values of  $\phi$  can be summarized in the following table:

Now, we can be say the series  $\sum_{k=0}^{\infty} \tilde{f}_k(\eta)$  converges to the solution  $\tilde{f}(\eta)$  when  $0 < \phi, \phi_1, \phi_2, \dots < 0$ .

**6. Results and Discussion**

Now, this section contains the discussions over different flow parameters on velocity profile  $\tilde{f}(\eta)$ . These parameters are Hartmann, Nano fluid volume fraction and Reynold numbers. Tables 3 and 4 show the convergence of B3. In Tables 5-8, the results of the imposed method are presented a compared with the numerical solution and the collocation method solution. These tables clearly indicate that the solutions are completely compatible. This accuracy gives high confidence to us about validity of this problem and reveals an excellent agreement of engineering accuracy. This investigation is completed by depicting the effects of some important parameters to evaluate how these parameters influence the fluid. The effect different values of active parameters is shown in Figures 2-4.

Figure 2. Follow for Material  $Al_2O_3$ .

In Figure 2a the effect of Hartmann number on the velocity profiles of divergent and convergent channels. The results show increasing Hartmann number leads to the velocity profiles of convergent and divergent channels is increased. So it can be seen by increasing Hartmann number that no backflow is occurred in both channels. Figure 2b shows that the fluid velocity decreases with Reynolds numbers in the case of divergent channels but increases with Reynold number in the case of convergent channels. Noticeably of all, by increasing nanofluid volume fraction, the fluid velocity decreases in the case of divergent channels but increases with nanofluid volume fraction in the case of convergent as depicted in Figure 2c.

Figure 3. Follow for Material  $TiO_2$ .

In Figure 3a, increasing Hartmann number on the velocity profiles of divergent and convergent channels is shown. This leads to decrease the velocity profiles of convergent and divergent channels. So in both channels, increasing Hartmann number no backflow is occurred. Figure 3b shows that the fluid velocity decreases with Reynolds numbers in the case of divergent and convergent channels. By increasing nanofluid volume fraction, the fluid velocity decreases in the case of divergent channels but decreases with nanofluid volume fraction in the case of convergent as depicted in Figure 3c.



**Table 5.** The profile of  $f(\eta)$  for Cu when  $Ha = 0, Re = 50, \alpha = 5, \phi = 0$ .

$\eta$	Present solution	HPM [12]	Reference [13]	Reference [23]	SHPM [12]	RK ~ 4
0.00	1.000000	1.000000	1.000000	1.000000	1.000000	1.000000
0.25	0.894649	0.894960	0.894242	0.894243	0.894242	0.894650
0.50	0.628312	0.627220	0.266948	0.626953	0.626948	0.628384
0.75	0.303771	0.302001	0.301991	0.301998	0.301990	0.304761
1.00	0.000000	0.000000	0.000000	0.000000	0.000000	0.000000

**Table 6.** The profile of  $f(\eta)$  for Cu when  $Ha = 750, Re = 10, \alpha = -5, \phi = 0.05$ .

$\eta$	Present solutions	Collocation method [9]
0.00	1.000000000	1.000000000
0.10	0.994237767	0.994278317
0.20	0.976518907	0.976670165
0.30	0.945519431	0.945855446
0.40	0.898941811	0.899546175
0.50	0.833382035	0.834341990
0.60	0.744151771	0.745536091
0.65	0.688792461	0.690394661
0.70	0.625067799	0.626869073
0.75	0.551934739	0.553888111
0.80	0.468230004	0.470248161
0.85	0.372665147	0.374605389
0.90	0.263823428	0.265469361
0.95	0.140159099	0.141198775
1.00	0.000000000	0.000000000

**Table 7.** The profile of  $f(\eta)$  for Cu when  $Ha = 600, Re = 30, \alpha = 5, \phi = 0.02$ .

$\eta$	Present solutions	RK ~ 4	Absolute error
0	1	1	0
0.05	0.997316914	0.997316914	$5.0 \times 10^{-10}$
0.1	0.989837623	0.989831339	0.989838538
0.2	0.959481313	0.959484798	0.959484798
0.3	0.909286554	0.909293747	0.909273894
0.4	0.839725036	0.839713174	0.839736189
0.5	0.751210824	0.751225047	0.751200975
0.6	0.643867387	0.643882692	0.643859464
0.7	0.51723661	0.517250595	0.51722988
0.75	0.446299608	0.446312228	0.446293494
0.8	0.369919206	0.369930217	0.369913902
0.85	0.287698312	0.287707601	0.287693905
0.9	0.199115412	0.199122776	0.199111677
0.95	0.103499625	0.103504315	0.103504315
1	0	0	0

**Table 8.** The profile of  $f(\eta)$  for  $Al_2O_3$  when  $Ha = 0, Re = 10, \alpha = 3, \phi = 0.01$ .

$\eta$	Present solutions	Numerical method [9]	Collocation method [9]
0.10	0.9892747583	0.9892747583	$2.10 \times 10^{-9}$
0.15	0.975894713	0.975894718	$5.00 \times 10^{-9}$
0.2	0.957211638	0.957211647	$9.00 \times 10^{-9}$
0.25	0.933273423	0.933273437	$1.44 \times 10^{-8}$
0.3	0.904140089	0.904140111	$2.20 \times 10^{-8}$
0.35	0.869882653	0.869882686	$3.32 \times 10^{-8}$
0.4	0.830581769	0.830581821	$5.20 \times 10^{-8}$
0.45	0.78632617	0.786326255	$8.54 \times 10^{-8}$
0.5	0.737210915	0.73721106	$1.45 \times 10^{-7}$
0.55	0.683335479	0.683335727	$2.41 \times 10^{-7}$
0.6	0.624801686	0.624802106	$4.19 \times 10^{-7}$
0.65	0.561711523	0.561712214	$6.91 \times 10^{-7}$
0.7	0.494164834	0.494165934	$1.10 \times 10^{-6}$
0.75	0.422256931	0.422258619	$1.68 \times 10^{-6}$
0.8	0.346076117	0.346078608	$2.49 \times 10^{-6}$
0.85	0.265701137	0.265704674	$3.53 \times 10^{-6}$
0.9	0.181198571	0.181203403	$4.83 \times 10^{-6}$
0.95	0.092620147	0.092626497	$6.34 \times 10^{-6}$
1	0	0.0.000008010	$8.01 \times 10^{-6}$

Figure 4. Follow for Material Cu.

The influence of Hartmann number on the velocity profiles of divergent and convergent channels is shown in Figure 4a. Note that decreasing the velocity profiles of convergent and divergent channels with increasing Hartmann number. In addition, in both channels by increasing Hartmann number that no backflow is occurred and can be seen clearly. Figure 4b proves that the fluid velocity decreases with Reynolds numbers in the case of divergent channels but increases with Reynold number in the case of convergent channels. The increasing nanofluid volume fraction in the case of divergent channels leads to a decrease in fluid velocity but in the case of convergent increases with nanofluid volume fraction as depicted in Figure 4c. Physically, the influence of the Reynolds number on the velocity distribution are owing to increased viscosity leading to fluid motion resistance at the boundary, thus momentum boundary layer increases. The nanofluid volume fraction effects on velocity and illustrates a gradual decrease in velocity profile as nanofluid volume fraction increases. As depicted in this plot, when  $\phi = 0$  it





shows the transport of the fluid through the channel without nanofluid volume fraction. Nanofluid volume fraction effects on the fluid and reduces momentum boundary layer thickness due to the high energy exchange rate as fluid molecules move through the nonparallel channel. Channel opening angles effect on the divergent/convergent plate. To eliminate the occurrence of fluid backflow, relatively large open channel angles are utilized. The backflow occurrence is eliminated for the converging channel, but may occur in the diverging channel. High Reynolds number value in the presence of high magnetic field intensity eliminates backflow phenomenon occurrence. As depicted, quantitative increase in the channels angle illustrates a significant decrease in the velocity profile. Magnetic field influences flow which shows magnetic field intensity and depicts that fluid flow decreases through the nonparallel channel. As observed from the plot, absolute velocity reduces, this can be explained physically due to the presence of resistive forces at the boundary of the channel due to boundary layer thickness increase resulting in retarding force on the velocity field.

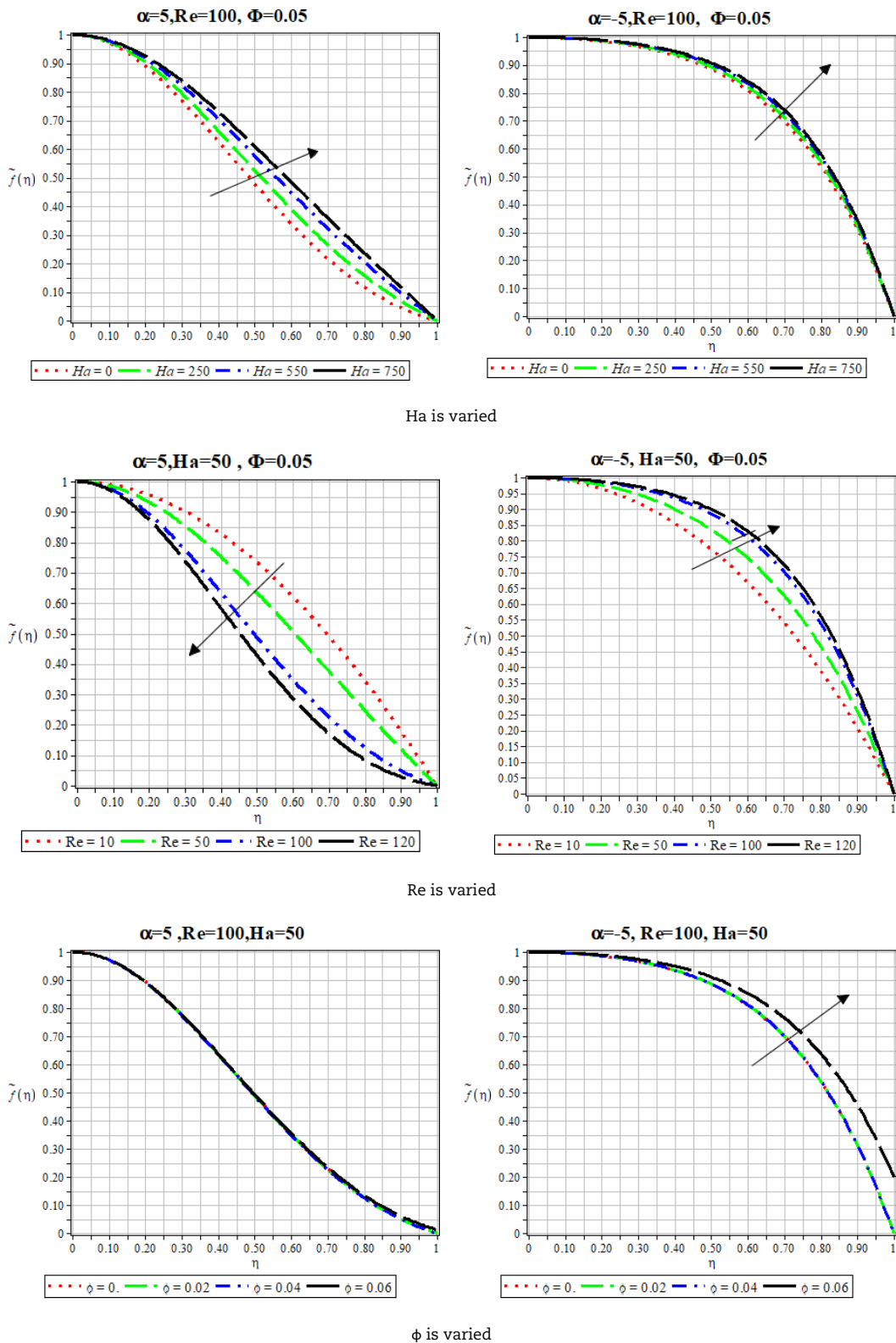


Fig. 2. The behavior of the velocity  $f(\eta)$  for  $\text{Al}_2\text{O}_3$ .



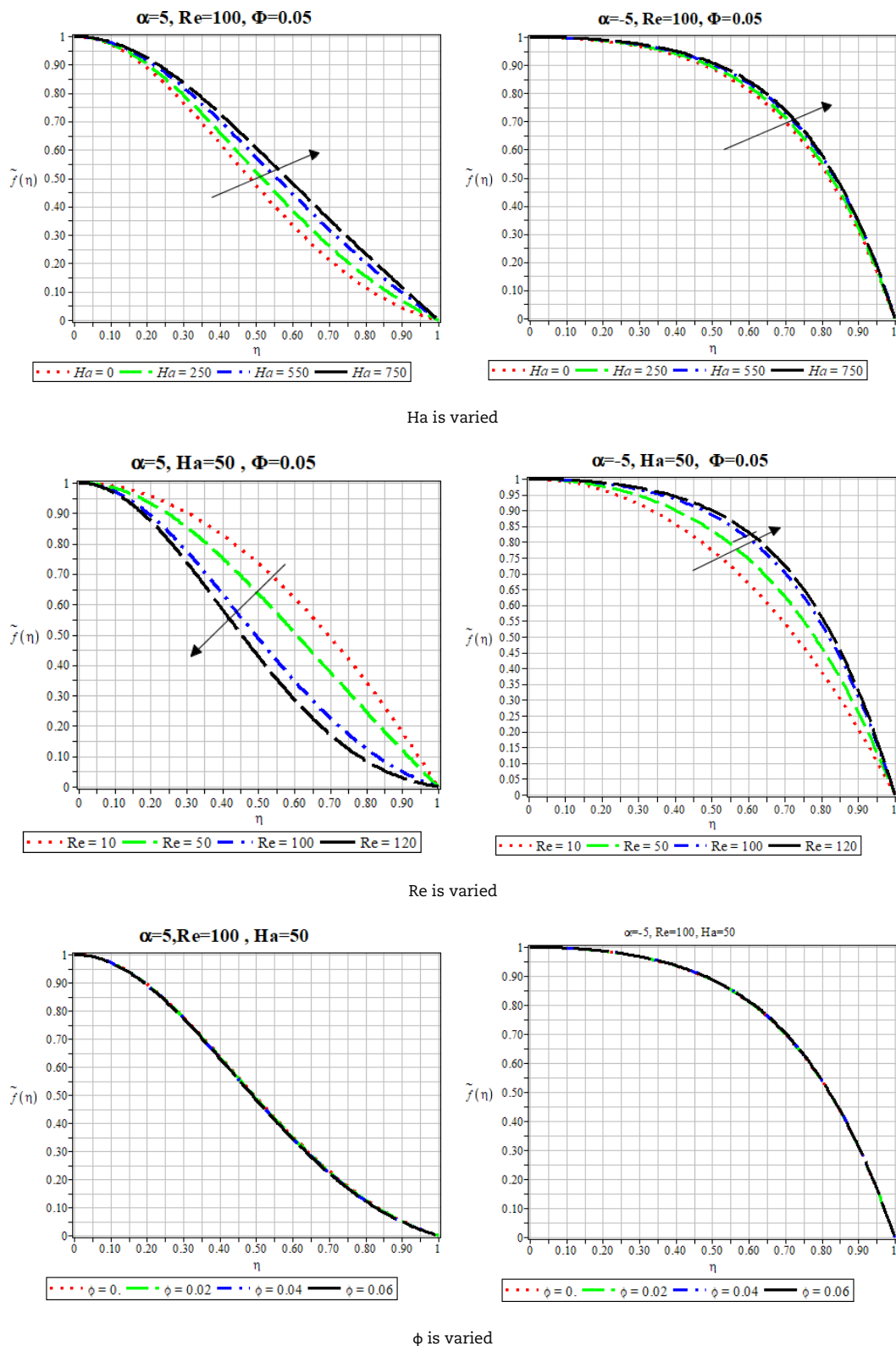


Fig. 3. The behavior of the velocity  $f(\eta)$  for  $\text{TiO}_2$ .

### 7. Conclusion

In this investigation, an analytical approach called NAM has been successfully applied to find the most accurate analytical solution for the velocity distributions of MHD Jeffery-Hamel problem with nanoparticles. The governing equations, continuity and momentum for this problem are reduced to an ordinary single third form by using a similarity transformation. Furthermore, the obtained solutions by proposed methods have been compared with the direct numerical solutions generated by RK ~ 4. The following main points can be concluded from the present study:

- New technique is a powerful approach for solving MHD Jeffery Hamel flow in high magnetic field with nanoparticles. It does



not need to any perturbation, linearization or small parameter versus Homotopy Perturbation Method (HPM) and Parameter Perturbation Method (PPM). Also, it does not need to determine the auxiliary parameter and auxiliary function versus Homotopy Analysis Method (HAM).

- Increasing Reynolds numbers leads to reduce velocity and excluded backflow in convergent channel.
- In greater angles, increasing Hartmann number will lead to no backflow increases.
- The channel is divergent; increasing nanofluid volume fraction will lead to the fluid velocity decrease. As for the converged channel, it is opposite to the state of divergent channel and has little effect.

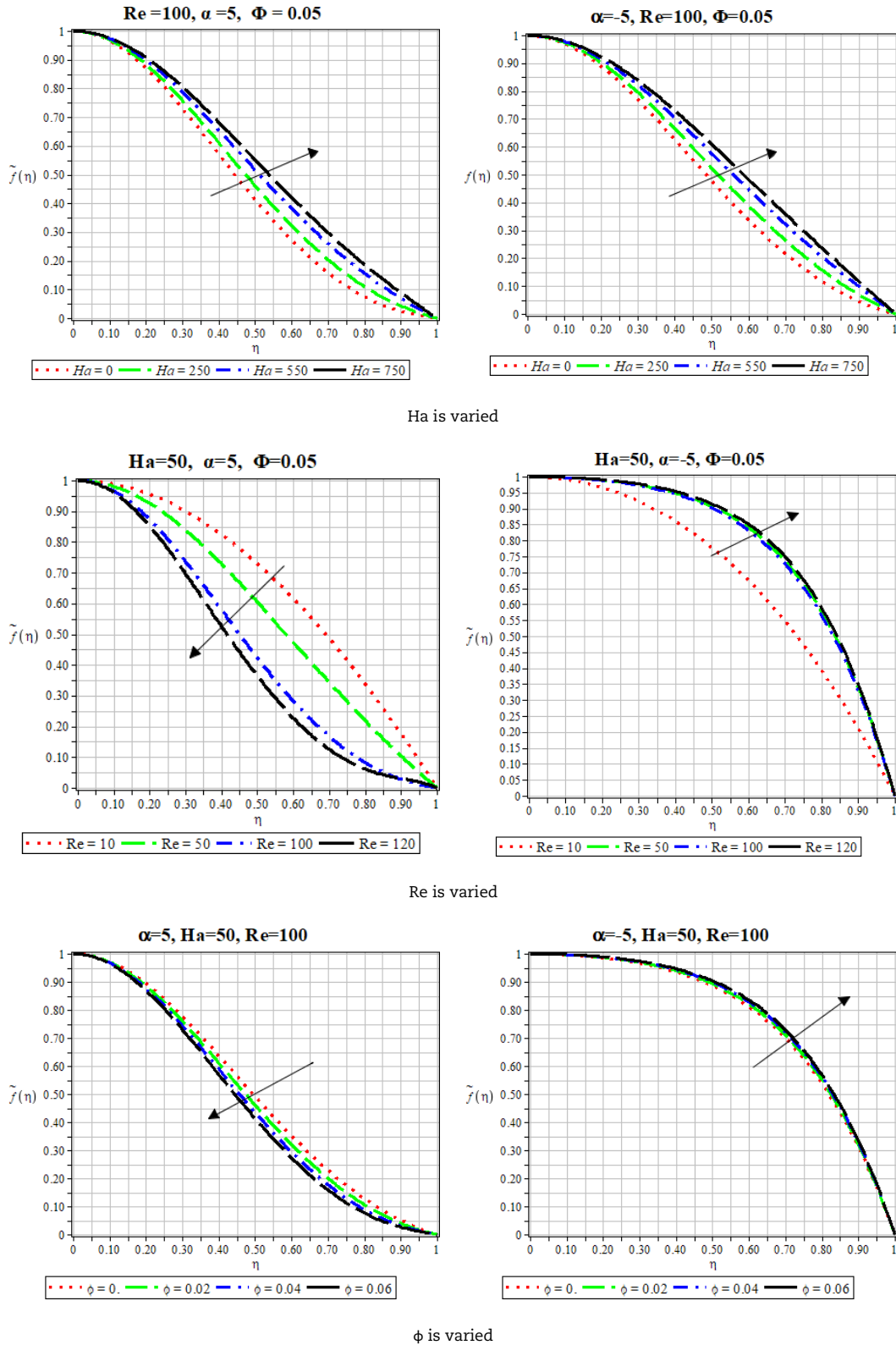


Fig. 4. The behavior of the velocity  $f(\eta)$  for Cu.



## Acknowledgments

The author is thankful to the anonymous reviews and editor for the valuable comments that helped to improve the quality of the presented work.

## Conflict of Interest

The author declared no potential conflicts of interest with respect to the research, authorship, and publication of this article.


## Funding

The author received no financial support for the research, authorship, and publication of this article.

## References

- [1] Jeffery, G.B., The two-dimensional steady motion of a viscous fluid, *Philos. Mag.*, 1915, 6, 45565.
- [2] Hamel, G., Bewegungen Spiralformige, Flussigkeiten Zaher, DersDeutschen Jahresbericht, *Math. Ver.*, 25, 1916, 34-60.
- [3] Nayfeh, A.H., *Perturbation methods*, New York, USA, Wiley, 2000.
- [4] Sheikholeslami, M., Ganji D.D., Ashorynejad, H.R., Rokni, H.B., Analytical investigation of Jeffery Hamel flow with high magnetic field and nanoparticle by Adomian decomposition method, *Appl. Math. Mech.*, 33(11), 2012, 25-36.
- [5] He, J.H., New interpretation of homotopy-perturbation method, *Int. J. Mod. Phys. B*, 20, 2006, 2561-8.
- [6] Moghimi, S.M., Ganji, D.D., Barmnia, H., Hosseini, M., Jalaal, M., Homotopy perturbation method for nonlinear MHD Jeffery Hamel problem, *Adv. Eng. Soft.*, 42, 2011, 108-113.
- [7] Rahimi Petroudi, I., Ganji, D.D., Shotorban, A.B., Khazayi Nejad, Ganji, N., Rahimi, E., Rohollahtabar, R., Taherinia, F., Semi analytical method for solving nonlinear equation arising of natural convection porous fin, *Therm. Sci.*, 16(5), 2012, 13-38.
- [8] Ganji, Z.Z., Ganji, D.D., Esmailpour, M., Study on nonlinear Jeffery Hamel flow by He's semi-analytical methods and comparison with numerical results, *Comput. Math. Appl.*, 58(1112), 2009, 2107-2116.
- [9] Rahimi Petroudi, I., Ganji, D.D., Khazayi Nejad, M., Rahimi, J., Rahimi, E., Rahimifar, A., Transverse magnetic field on Jeffery-Hamel problem with Cu-water nanofluid between two nonparallel plane walls by using collocation method, *Case Studies in Thermal Engineering*, 4, 2014, 193-201.
- [10] Ganji, D.D., Azimi, M., Application of DTM on MHD Jeffery Hamel problem with nanoparticles, *U.P.B. Sci. Bull. Ser. A*, 6, 2013, 75-81.
- [11] Abbasi, M., Ganji, D.D., Rahimi Petroudi, I., Khaki, M., Comparative analysis of MHD boundary-layer flow of viscoelastic fluid in permeable channel with slip boundaries by using HAM, VIM, HPM, *Walailak J. Sci. Tech.*, 11(7), 2014, 55167.
- [12] Khidir, A.A., A new spectral homotopy perturbation method and its application to Jeffery-Hamel nanofluid flow with high magnetic field, *Journal of Computational Method in Physics*, 2013, 2013, 10 pages.
- [13] Motsa, S.S., Sibanda, P.F., Awad, G., Shateyi, S., A new spectral-homotopy analysis method for the MHD Jeffery-Hamel problem, *Computers and Fluids*, 39(7), 2010, 1219-1225.
- [14] Al-Saif, A.J.A., Jasim, A.M., A new analytical-approximate solution for the viscoelastic squeezing flow between two parallel plates, *Applied Mathematics and Information Sciences*, 13(2), 2019, 173-182.
- [15] Al-Saif, A.J.A., Jasim, A.M., A novel algorithm for studying the effects of squeezing flow of a Casson Fluid between parallel plates on magnetic field, *Journal of Applied Mathematics*, 2019, 2019, 3679373.
- [16] Al-Saif, A.J.A., Jasim, A.M., New Analytical Study of the Effects Thermo- Diffusion, Diffusion-Thermo and Chemical Reaction of Viscous Fluid on Magneto Hydrodynamics Flow in Divergent and Convergent Channels, *Applied Mathematics*, 10, 2019, 268300.
- [17] Al-Saif, A.J.A., Jasim, A.M., Analytical Investigation of the MHD Jeffery-Hamel Flow Through Convergent and Divergent Channel by New Scheme, *Engineering Letters*, 27(3), 2019, 27-3-28.
- [18] Jasim, A.M., Al-Saif, A.J.A., New Analytical Solution Formula for Heat Transfer of Unsteady Two-Dimensional Squeezing Flow of a Casson Fluid between Parallel Circular Plates, *Journal of Advanced Research in Fluid Mechanics and Thermal Sciences*, 64(2), 2019, 219-243.
- [19] Jasim, A.M., Analytical approximation of the first grade MHD squeezing fluid flow with slip boundary condition using a new iterative method, *Heat Transfer*, 10, 2020, 1-21.
- [20] Sheikholeslami, M., Jafaryar, M., Said, Z., Alsabery, A., Babazadeh, H., Shafee, A., Modification for helical turbulator to augment heat transfer behavior of nanomaterial via numerical approach, *Applied Thermal Engineering*, 2020, DOI: 10.1016/j.applthermaleng.2020.115935.
- [21] Sheikholeslami, M., Farshad, S.A., Shafee, A., Babazadeh, H., Influence of Al<sub>2</sub>O<sub>3</sub> nano power on performance of solar collector considering turbulent flow, *Advanced Powder Technology*, 2020.
- [22] Sheikholeslami, M., Farshad, S.A., Shafee, A., Babazadeh, H., Performance of solar collector with turbulator involving nanomaterial turbulent regime, *Renewable Energy*, 163, 2021, 1222-1237.
- [23] Ganji, Z.Z., Ganji, D.D., Esmailpour, M., Study on nonlinear Jeffery- Hamel flow by He's semi-analytical methods and comparison with numerical results, *Computers and Mathematics with Applications*, 58(12), 2009, 2107-2116.
- [24] Petroudi, I.R., Ganji, D.D., Nejad, M.K., Rahimi, J., Rahimi, E., Rahimifar, A., Transverse magnetic field on Jeffery-Hamel problem with Cu-water nanofluid between two non-parallel plane walls by using collocation method, *Case Studies in Thermal Engineering*, 4, 2014, 193-201.
- [25] Akinbowale, T.A., Adeleke, I., Hafiz M.A., Abdul-Jalil S., Heat transfer analysis of nanofluid flow with porous medium through Jeffery Hamel diverging/converging channel, *J. Appl. Comput. Mech.*, 6(3) 2020, 433-444.

## ORCID iD

Abeer Majeed Jasim  <https://orcid.org/0000-0001-6713-5696>



© 2020 by the authors. Licensee SCU, Ahvaz, Iran. This article is an open access article distributed under the terms and conditions of the Creative Commons Attribution-NonCommercial 4.0 International (CC BY-NC 4.0 license) (<http://creativecommons.org/licenses/by-nc/4.0/>).

How to cite this article: Jasim, A.M. New Analytical Study for Nanofluid between Two Non-Parallel Plane Walls (Jeffery-Hamel Flow), *J. Appl. Comput. Mech.*, 7(1), 2021, 213–224. <https://doi.org/10.22055/JACM.2020.34958.2520>

